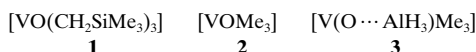


- [9] *New Vaccine Development: Establishing Priorities. Vol. 2. Diseases of Importance in Developing Countries*, National Academy Press, Washington, DC, **1986**, pp. 329–337.
- [10] The term “oligosaccharide” is used in a liberal manner to denote the saccharides described here, while cognizant of the fact that by definition (Joint Commission on Biological Nomenclature, *Eur. J. Biochem.* **1982**, 126, 433–437.) oligosaccharides contain up to and including ten monosaccharide units.
- [11] a) V. Pozsgay, B. Coxon, *Carbohydr. Res.* **1995**, 277, 171–178; b) V. Pozsgay, L. Pannell, *ibid.* **1994**, 258, 105–122; c) V. Pozsgay, B. Coxon, *Carbohydr. Res.* **1994**, 257, 189–215; d) V. Pozsgay, B. Coxon, H. Yeh, *Bioorg. Med. Chem.* **1993**, 1, 237–257; e) V. Pozsgay, C. P. J. Glaudemans, J. B. Robbins, R. Schneerson, *Carbohydr. Res.* **1993**, 244, 259–273; f) V. Pozsgay, C. P. J. Glaudemans, J. B. Robbins, R. Schneerson, *Tetrahedron* **1992**, 48, 10249–10264.
- [12] In one unpublished approach, a pentamer of a tetrasaccharide, similar to **14** was constructed, except that it contained an azido function at C-2 of the glucose unit. Various attempts to convert that protected eicosasaccharide to the corresponding acetamido derivative led to inseparable, complex mixtures.
- [13] All new compounds gave satisfactory elemental analytical and mass spectral data. Yields refer to chromatographically homogeneous material.
- [14] H. Lönn, *Carbohydr. Res.* **1985**, 139, 105–113.
- [15] a) V. Pozsgay in *Carbohydrates, Synthetic Methods and Applications in Medicinal Chemistry* (Eds.: H. Ogura, A. Hasegawa, T. Suami), Kodansha-VCH, Tokyo, Weinheim, **1992**, pp. 188–227; b) H. Paulsen, C. Krogmann, *Liebigs Ann. Chem.* **1989**, 1203–1213; c) M. Imoto, H. Yoshimura, T. Shimamoto, N. Sakaguchi, T. Shiba, *Bull. Chem. Soc. Jpn.* **1987**, 60, 2205–2214; d) T. B. Windholz, D. B. R. Johnston, *Tetrahedron Lett.* **1967**, 2555–2557.
- [16] Y. Oikawa, T. Yoshioko, O. Yonemitsu, *Tetrahedron Lett.* **1982**, 23, 885–888.
- [17] a) P. Konradsson, U. E. Udodong, B. Fraser-Reid, *Tetrahedron Lett.* **1990**, 31, 4313–4316; b) G. H. Veeneman, S. H. van Leeuwen, J. H. van Boom, *ibid.* **1990**, 31, 1331–1334.
- [18] a) R. R. Schmidt, J. Michel, *Angew. Chem.* **1980**, 92, 763–764; *Angew. Chem. Int. Ed. Engl.* **1980**, 19, 731–732; b) M. Numata, M. Sugimoto, K. Koike, T. Ogawa, *Carbohydr. Res.* **1987**, 163, 209–225; c) review: R. R. Schmidt, W. Kinzy, *Adv. Carbohydr. Chem. Biochem.* **1994**, 50, 21–123.
- [19] L. Yan, D. Kahne, *J. Am. Chem. Soc.* **1996**, 118, 9239–9248.
- [20] Compound **22** was obtained from **15** (S. Sabesan, J. C. Paulson, *J. Am. Chem. Soc.* **1986**, 108, 2068–2080.) through a sequence involving oxidation (A. J. Mancuso, S. L. Huang, D. Swern, *J. Org. Chem.* **1978**, 43, 2480–2482.), acetalization [(MeO)₂CMe₂, CSA], ester hydrolysis (LiOH), and acidification (citric acid) in 78% overall yield.
- [21] For our earlier approaches for the introduction of a terminal, aldehyde group-containing linker moiety, see a) V. Pozsgay, L. Trinh, J. Shiloach, J. B. Robbins, A. Donahue Rolfe, S. B. Calderwood, *Bioconj. Chem.* **1996**, 7, 45–55. b) V. Pozsgay, *Glycoconj. J.* **1993**, 10, 133–141.
- [22] G. R. Gray, *Arch. Biochem. Biophys.* **1974**, 163, 426–428. Reductive amination attaches the ω -aldehydealkyl moiety to the ϵ -amino group of the lysine residues of proteins resulting in an ϵ -N-alkylated construct that preserves the original net charge of the protein (C. P. Stowell, Y. C. Lee, *Adv. Carbohydr. Chem. Biochem.* **1981**, 37, 225–281).
- [23] The MALDI-TOF mass spectra were recorded on a KRATOS MALDI III instrument operated at an accelerating voltage of 22 kV. The sample was dissolved in 0.1% trifluoroacetic acid and 50% acetonitrile and applied to the target sample in a sinapinic acid matrix. The molecular weight of HSA was measured as 66350 Da.

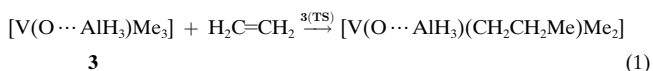
Correlation between ⁵¹V NMR Chemical Shift and Reactivity of Oxovanadium(V) Catalysts for Ethylene Polymerization**

Michael Bühl*

Olefin polymerization is one of the most important industrial applications of organometallic catalysts.^[1] The most widely used catalysts in both homo- and heterogeneous reactions are of the Ziegler type, that is, based on Ti and Zr species along with certain cocatalysts.^[2–4] The key step (not necessarily the rate-determining one) is the insertion of the olefin into a metal–carbon bond. Several such reactions and thus many potential catalysts for olefin polymerization are known. Silica-supported vanadium catalysts have attracted some attention in this context.^[5] The oxidation state of the active vanadium species is still being debated;^[5] low-valent species have been typically assumed, but studies on a soluble model compound have indicated that vanadium in the oxidation state V can also be catalytically active.^[6] Upon addition of alkylaluminum reagents the simpler model compound **1** also shows mild catalytic activity for ethylene polymerization.^[7] From multinuclear NMR spectroscopy it has been concluded that in the active catalyst, the organoaluminum compound is coordinated to the terminal oxygen atom of **1**.^[7]



Recent calculations for model systems **2** and **3**, employing gradient-corrected levels of density functional theory (DFT), have corroborated this conclusion and have outlined a plausible mechanism for ethylene polymerization by **3** [Eq. (1)].^[8] The rate-determining step is ethylene insertion into a V–C bond



via the transition structure **3(TS)**, which has approximate square–pyramidal coordination about the vanadium center.

The role of the cocatalyst is addressed here in more detail, and the dependence of the computed insertion barrier on the specific Lewis acid is examined. As the latter is also found to affect the chemical shifts of the reactant complex substantially, it is suggested that prospective cocatalysts may be identified by ⁵¹V NMR spectra of their adducts with, for example, **1**.

Apart from **3**, model catalysts [V(O⋯X)Me₃] derived by addition of Lewis acids X have been investigated: none (**2**), Li⁺ (**4**), SbF₅ (**5**), and H⁺ (**6**). Absolute and zero-point energies^[9,10] of reactant minima and transition states, as well as the resulting barriers are collected in Table 1, and the transition structures are displayed in Figure 1. As expected,

[*] Dr. M. Bühl
Organisch-chemisches Institut der Universität
Winterthurerstrasse 190, CH-8057 Zürich (Switzerland)
Fax: Int. code + (41) 1-635 6812
e-mail: buehl@oci.unizh.ch

[**] I thank Prof. W. Thiel for his continuous support. Calculations were performed on a Silicon Graphics PowerChallenge at the Organisch-chemisches Institut, on IBM RS/6000 workstations at the ETH Zürich (C4 cluster), and on a NEC-SX4 supercomputer at the CSCS in Manno (Switzerland).

Table 1. Absolute energies E_{tot} and zero-point energies (in square brackets) of reactants and transition states for the system $[\text{V}(\text{O}\cdots\text{X})\text{Me}_3] + \text{C}_2\text{H}_4$, insertion barriers ΔE_a (including BP86/AE1 zero-point corrections), and chemical shifts $\delta(^{51}\text{V})$ (with respect to $[\text{VOCl}_3]$) of the reactants.

Molecule	X	E_{tot} (minima) ^[a,b]	E_{tot} (TS) ^[a]	ΔE_a ^[c]	$\delta(^{51}\text{V})$ ^[d]
2	–	–1139.12352 [66.0]	–1217.67283 [101.5]	22.2	1062
3	AlH_3	–1383.34929 [78.5]	–1461.90418 [114.6]	19.1	1407
4	Li^+	–1146.46946 [66.7]	–1225.02605 [102.4]	17.8	1557
5	SbF_5	–1643.87993 [74.3]	–1722.43720 [109.6]	16.9	1766
6	H^+	–1139.44031 [70.8]	–1218.00770 [107.3]	11.9	1911

[a] BP86/I level; absolute energies in Hartree; ZPE in kcal mol^{–1}; each minimum has no imaginary frequency, each transition state has one imaginary frequency. [b] Values for ethylene at the same level are –78.57773 [31.2]. [c] (BP86/I + ZPE) level; in kcal mol^{–1}. [d] GIAO-B3LYP/I level for BP86/I geometries.

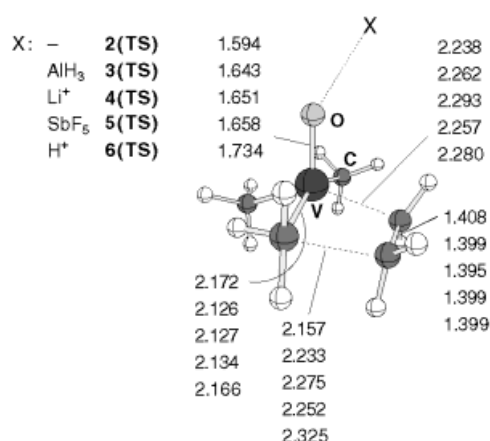


Figure 1. Transition structure for ethylene insertion into a V–C bond of **2** and Lewis adducts thereof; key distances are given in Å (BP86/I-optimized structures).

the uncatalyzed reaction (i.e. starting from **2**) has the highest computed insertion barrier, 22.2 kcal mol^{–1}. Addition of AlH_3 lowers the barrier by roughly 3 kcal mol^{–1}. Inspection of the natural charges^[11] and Wiberg bond indices^[12] in Figure 2 gives some information on the reason for this barrier reduction. As the coordination number at the vanadium atom is increased, in other words on going from the reactant **2** to the transition state **2(TS)**, the V–O bond order decreases and the negative charge on the oxygen atom increases. Both effects appear to be quite small, but they are somewhat more pronounced in the corresponding AlH_3 adducts. On going from **3** to **3(TS)** the negative charge on the oxygen atom increases by 13% and the V–O bond order decreases by 7% (Figure 2). Apparently, the Lewis acid stabilizes the negative charge on the oxygen atom more efficiently in the transition state than in the reactant complex, thereby lowering the overall barrier.

As a consequence, stronger Lewis acids should stabilize the transition structure even more effectively and should thus further reduce the barrier. For instance, with Li^+ as cocatalyst, a barrier of 17.8 kcal mol^{–1} is computed, more than 1 kcal mol^{–1} lower than that with AlH_3 (Table 1). Similar “electrostatic accelerations” have been predicted computationally for pericyclic reactions^[13] and are known experimentally (for instance, the rates of Diels–Alder and ene reactions

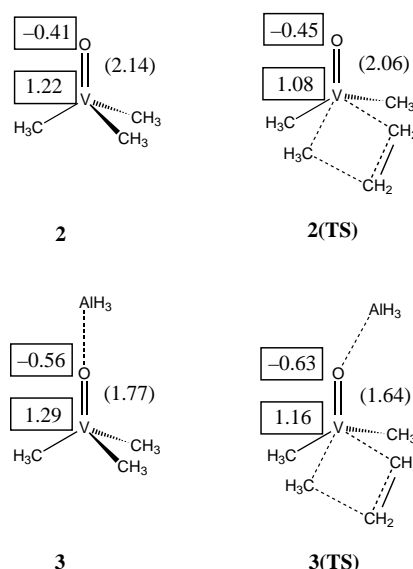


Figure 2. Natural charges (in boxes) and Wiberg bond orders (in parentheses) for **2**, **3**, and the corresponding transition structures for ethylene insertion (obtained from natural population analysis at the BP86/I level).

are enhanced by inorganic lithium salts^[14]). A further reduction of the barrier to 16.9 kcal mol^{–1} is predicted when SbF_5 is the cocatalyst. Finally, with one of the strongest acids conceivable, unsolvated H^+ , the computed barrier is only 11.9 kcal mol^{–1}. This result may be of little immediate relevance for chemistry in solution, but may serve as a rough estimate for the lower limit for the barrier that can be reached with this type of system. (Note that the theoretical numbers are not necessarily of quantitative accuracy; the computed trends, however, should be reliable.)

Complexation of the Lewis acid at the terminal oxygen atom affects not only the barrier, but also the chemical shifts of the oxovanadium(V) reactants. For instance, the ^{51}V signal of **1** is shifted to higher frequency by $\Delta\delta = 370$ upon coordination of $\text{Al}(\text{CH}_2\text{SiMe}_3)_3$.^[7] Similar deshielding, $\Delta\delta = 345$, is obtained on going from model system **2** to its AlH_3 adduct **3** (see Table 1). Moreover, successive deshielding of the ^{51}V nucleus is computed on proceeding from **2** to compounds **4**, **5**, and **6**, with a value of up to $\Delta\delta = 851$ for the latter (Table 1). This deshielding can be understood in terms of paramagnetic contributions due to magnetically induced coupling^[15] between the occupied V–C bonding MOs (one “ σ_{VC} ” and two “ π_{VC} ”) and the virtual, antibonding orbital, “ σ_{VO}^* ”. The latter is strongly stabilized upon protonation (on going from **2** to **6**), much more than the former. Hence, the energetic separation between both is reduced and the resulting paramagnetic contributions are enhanced.

As illustrated in Figure 3, the Lewis acid X affects both $\delta(^{51}\text{V})$ of the reactants and the insertion barrier in a similar way. While there is no strictly linear relationship between these two properties, the general trend is obvious: enhanced deshielding of the ^{51}V nucleus is paralleled by a decrease of the insertion barrier.

There are several reports of empirical correlations of transition metal chemical shifts with kinetic parameters^[16] and, in some cases, even with catalytic activities.^[17,18] Such

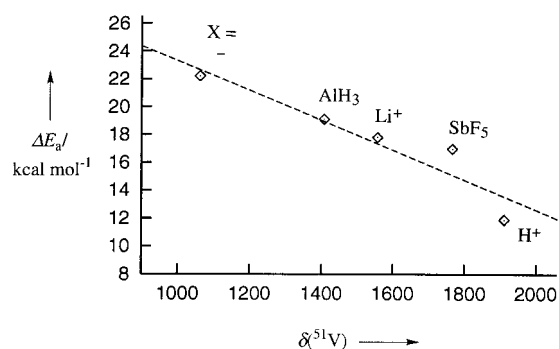


Figure 3. Correlation of DFT-derived barriers to ethylene insertion ΔE_a (BP86/I + ZPE) and chemical shifts $\delta(^{51}\text{V})$ (GIAO-B3LYP/I) for the Lewis acid adducts $[\text{V}(\text{O} \cdots \text{X})\text{Me}_3]$.

correlations are potentially very useful because reactivities of new compounds can be estimated from the NMR spectra alone. In some cases, DFT calculations have reproduced and rationalized the experimental findings.^[19] The results summarized in Figure 3 constitute the first theoretical prediction of such a NMR–reactivity correlation. When applied to the experimental system **1**, these data indicate that the polymerization activity towards ethylene may be increased by Lewis acids stronger than the alkylaluminum reagents employed so far.^[7] Most significantly, it should be possible to screen suitable cocatalysts by recording ^{51}V NMR spectra of the complexes formed initially with **1**:^[20] the complexes with the most deshielded $\delta(^{51}\text{V})$ resonance should also be the most reactive ones. If the lower limit of the ethylene insertion barrier is around 12 kcal mol^{−1} as computed for **6** (with H⁺ as cocatalyst), catalysts derived from **1** can most likely not match the high activity of the Kaminsky-type zirconocenes, for which propagation barriers on the order of 7 kcal mol^{−1} have been estimated.^[21] Nevertheless, it would be very interesting to test experimentally whether the catalytic activity of **1** can be significantly increased by suitable cocatalysts, and whether the predicted NMR–reactivity correlation of Figure 3 can be verified (provided possible problems with the solubility and stability of potential catalysts can be overcome).

Received: July 9, 1997 [Z10658IE]
German version: *Angew. Chem.* **1998**, *110*, 153–155

Keywords: density functional calculations • homogeneous catalysis • NMR spectroscopy • polymerization • vanadium

- [1] a) *Applied Homogeneous Catalysis with Organometallic Compounds, Vol. 1,2* (Eds.: B. Cornils, W. A. Herrmann), VCH, Weinheim, **1996**; b) W. A. Herrmann, B. Cornils, *Angew. Chem.* **1997**, *109*, 1074–1095; *Angew. Chem. Int. Ed. Engl.* **1997**, *36*, 1049–1067.
- [2] K. Ziegler, *Angew. Chem.* **1964**, *76*, 545–566.
- [3] J. Boor Jr., *Ziegler–Natta Catalysts and Polymerizations*, Academic Press, New York, **1979**.
- [4] H. H. Brintzinger, D. Fischer, R. Mühlhaupt, B. Rieger, R. Waymouth, *Angew. Chem.* **1995**, *107*, 1255–1283; *Angew. Chem. Int. Ed. Engl.* **1995**, *34*, 1143.
- [5] See for example: F. J. Karol, K. J. Cann, B. E. Wagner in *Transition Metals and Organometallics as Catalysts for Olefin Polymerization* (Eds.: W. Kaminsky, H. Sinn), Springer, New York, **1988**, p. 149.
- [6] F. J. Feher, R. L. Blanski, *J. Am. Chem. Soc.* **1992**, *114*, 5886–5887.
- [7] F. J. Feher, R. L. Blanski, *Organometallics* **1993**, *12*, 958–963.

- [8] M. Bühl, F. A. Hamprecht, *J. Comput. Chem.*, in press.
- [9] Method for geometry optimization: gradient-corrected exchange-correlation functionals of Becke (A. D. Becke, *Phys. Rev. A* **1988**, *38*, 3098–3100) and Perdew (J. P. Perdew, *Phys. Rev. B* **1986**, *33*, 8822–8824; *ibid.* **1986**, *34*, 7406), denoted BP86, and Basis I, which is Wachters's (14s11p6d)/[8s7p4d] all-electron basis augmented with one additional diffuse d function and two 4p functions for V (A. J. H. Wachters, *J. Chem. Phys.* **1970**, *52*, 1033–1036; P. J. Hay, *J. Chem. Phys.*, **1977**, *66*, 4377–4384), a relativistic 64-electron multi-electron-fit effective core potential together with the (4s4p)/[2s2p] valence double-zeta basis set for Sb (A. Bergner, M. Dolg, W. Küchle, H. Stoll, H. Preuss, *Mol. Phys.* **1993**, *80*, 1431–1441; augmented with one d-polarization function, exponent 0.211), and standard 6-31G* basis for all other elements (e.g. W. Hehre, L. Radom, P. von R. Schleyer, J. A. Pople, *Ab Initio Molecular Orbital Theory*, Wiley, New York, **1986**). Zero-point corrections have been computed with harmonic frequencies from analytical or numerical second derivatives. It is known that these types of density functionals afford reliable descriptions of geometries, vibrations, and energetics for transition metal complexes (see, for example, T. Ziegler, *Can. J. Chem.* **1995**, *73*, 743–761).
- [10] Magnetic shieldings have been computed with the GIAO (Gauge-Including Atomic Orbitals) DFT method as implemented (J. R. Cheeseman, G. W. Trucks, T. A. Keith, M. J. Frisch, *J. Chem. Phys.* **1996**, *104*, 5497–5509) in the Gaussian 94 program (M. J. Frisch, G. W. Trucks, H. B. Schlegel, P. M. W. Gill, B. G. Johnson, M. A. Robb, J. R. Cheeseman, T. Keith, G. A. Petersson, J. A. Montgomery, K. Raghavachari, M. A. Al-Laham, V. G. Zakrzewski, J. V. Ortiz, J. B. Foresman, C. Y. Peng, P. Y. Ayala, W. Chen, M. W. Wong, J. L. Andres, E. S. Replogle, R. Gomperts, R. L. Martin, D. J. Fox, J. S. Binkley, D. J. DeFrees, J. Baker, J. J. P. Stewart, M. Head-Gordon, C. Gonzales, J. A. Pople, Gaussian 94, Pittsburgh PA, 1995), employing Basis I and Becke's three-parameter exchange DFT/Hartree–Fock hybrid functional (A. D. Becke, *J. Chem. Phys.* **1993**, *98*, 5648–5642) together with the correlation functional of Lee, Yang, and Parr (C. Lee, W. Yang, R. G. Parr, *Phys. Rev. B* **1988**, *37*, 785–789), denoted B3LYP, for the BP86/I-optimized geometries. Chemical shifts are reported relative to $[\text{VOCl}_3]$, the experimental standard, with a computed absolute shielding of $\sigma = -2317$ at the same level.^[8] It is not mandatory that geometry optimizations and chemical shift calculations be performed at the same level. For the computation of some transition metal chemical shifts, the B3LYP functional has proven superior to others (M. Bühl, *Chem. Phys. Lett.* **1997**, *267*, 251–257); see also ref.^[8]
- [11] From natural population analysis; review: A. E. Reed, L. A. Curtiss, F. Weinhold, *Chem. Rev.* **1988**, *88*, 899–926.
- [12] K. Wiberg, *Tetrahedron* **1968**, *24*, 1083–1096.
- [13] a) H. Jiao, P. von R. Schleyer, *Angew. Chem.* **1993**, *105*, 1830–1833; *Angew. Chem. Int. Ed. Engl.* **1993**, *32*, 1760–1763; b) H. Jiao, P. von R. Schleyer, *J. Am. Chem. Soc.* **1995**, *117*, 11529–11535.
- [14] See for example: G. Facita, P. Righetti, *Tetrahedron* **1995**, *51*, 9091–9102.
- [15] For the origin of paramagnetic contributions see, for example: W. Kutzelnigg, U. Fleischer, M. Schindler, in *NMR Basic Princ. Prog.* **1990**, *23*, 165–262; an illustration for transition metal complexes can be found in, for example, Y. Ruiz-Morales, G. Schreckenbach, T. Ziegler, *J. Phys. Chem.* **1996**, *100*, 3359–3367.
- [16] See for example: a) P. DeShong, D. R. Sidler, P. J. Rybczynski, A. A. Ogilvie, W. von Philipsborn, *J. Org. Chem.* **1989**, *54*, 5432–5437; b) M. Koller, W. von Philipsborn, *Organometallics* **1992**, *11*, 467–468; c) M. Koller, Ph.D. Thesis, Universität Zurich, **1993**; d) E. J. Meier, W. Kozminski, A. Linden, P. Lustenberger, W. von Philipsborn, *Organometallics* **1996**, *15*, 2469–2477.
- [17] H. Bönemann, W. Brijoux, R. Brinkmann, W. Meurers, R. Mynott, W. von Philipsborn, T. Egolf, *J. Organomet. Chem.* **1984**, *272*, 231–249.
- [18] R. Fornika, H. Görls, B. Seeman, W. Leitner, *J. Chem. Soc. Chem. Commun.* **1995**, 1479–1480.
- [19] a) M. Bühl, O. L. Malkina, V. G. Malkin, *Helv. Chim. Acta* **1996**, *79*, 742–754; b) M. Bühl, *Organometallics* **1997**, *16*, 261–267.
- [20] No NMR spectra are necessary to order possible cocatalysts according to their Lewis acid strength, but rather to ensure that stable complexes are formed in each case.
- [21] J. C. W. Chien, A. Razavi, *J. Polym. Sci. A* **1988**, *26*, 2369–2380.